
NeuraCrypt: Hiding Private Health Data via Random Neural Networks for Public Training

Adam Yala^{†*}, Homa Esfahanizadeh^{†*}, Rafael G. L. D’Oliveira[†], Ken R. Duffy[‡],

Manya Ghobadi[†], Tommi S. Jaakkola[†], Vinod Vaikuntanathan[†]

Regina Barzilay[†], Muriel Médard[†]

[†]Massachusetts Institute of Technology (MIT), 02139 USA

[‡]Maynooth University, Ireland

{adamyala, ghobadi, tommi, regina}@csail.mit.edu

{homaesf, rafaeld, vinodv, medard}@mit.edu

Ken.Duffy@mu.ie

Abstract

Balancing the needs of data privacy and predictive utility is a central challenge for machine learning in healthcare. In particular, privacy concerns have led to a dearth of public datasets, complicated the construction of multi-hospital cohorts and limited the utilization of external machine learning resources. To remedy this, new methods are required to enable data owners, such as hospitals, to share their datasets publicly, while preserving both patient privacy and modeling utility. We propose *NeuraCrypt*², a private encoding scheme based on random deep neural networks. *NeuraCrypt* encodes raw patient data using a randomly constructed neural network known only to the data-owner, and publishes both the encoded data and associated labels publicly. From a theoretical perspective, we demonstrate that sampling from a sufficiently rich family of encoding functions offers a well-defined and meaningful notion of privacy against a computationally unbounded adversary with full knowledge of the underlying data-distribution. We propose to approximate this family of encoding functions through random deep neural networks. Empirically, we demonstrate the robustness of our encoding to a suite of adversarial attacks and show that *NeuraCrypt* achieves competitive accuracy to non-private baselines on a variety of x-ray tasks. Moreover, we demonstrate that multiple hospitals, using independent private encoders, can collaborate to train improved x-ray models. Finally, we release a challenge dataset³ to encourage the development of new attacks on *NeuraCrypt*.

*Equal contribution

²github.com/yala/NeuraCrypt

³github.com/yala/NeuraCrypt-Challenge

1 Introduction

One of the central challenges of developing machine learning tools in healthcare is access to patient data. To protect patients’ privacy, regulations such as HIPAA [HIPAA] and GDPR [GDPR] greatly complicate creation of large, multi-institutional datasets, a necessary resource for training robust and equitable models. Consequently, the lack of public datasets has excluded the broad machine learning research community from contributing to clinical AI. Addressing this challenge is the focus of our paper. Consider the scenario where a hospital wishes to publicly release a dataset of mammograms with cancer labels. We are interested in developing a computationally effective mechanism for image encoding that both protects patient privacy (i.e., hiding the correspondence between patients and encoded samples), and facilitates learning.

There are a number of solutions that have been developed for different notions of privacy. While federated learning [McMahan et al., 2017] can offer privacy by training models in a distributed fashion, the framework relies on the coordination of data owners and model developers to run shared software. This framework is not designed to enable hospitals to deposit their datasets publicly. Cryptographic methods, such as secure multi-party computation, fully homomorphic encryption and functional encryption [Gentry, 2009, Brakerski and Vaikuntanathan, 2011, Boneh et al., 2012, Cho et al., 2018] could enable such public sharing and offer extremely strong security guarantees, hiding everything about the data. However, these security guarantees come at the cost of high computational overheads for use with modern methods. The notion of security adopted by these cryptographic methods is not suited to our setting, where image labels are public. Instead, we seek an efficient encoding scheme to protect the information not already implied by the image label.

We propose *NeuraCrypt*, a private encoding scheme designed to enable data owners to publish their data publicly while preserving both data privacy and modeling utility. *NeuraCrypt* encodes raw patient data using a randomly constructed neural network, known only to the data owner, and deposits both the encoded data and associated labels publicly for unknown third parties to develop models. When applied in the multi-institutional setting, each site utilizes independent private encoders to encrypt their data. With the help of label information, models trained in this setting can map these independently constructed encodings into a shared feature space. While the data remains private across the sites, each institution can still benefit from the larger combined dataset.

Our design is guided by theoretical considerations. First, we demonstrate a means, albeit an inefficient one, of offering for each sample anonymity amongst all other possible samples sharing the same label. Our approach relies on random selection of an encoder from a sufficiently rich family of encoding functions. Secondly, while we cannot construct the optimal family of encoding functions directly, i.e. all possible bijections, we demonstrate that we can iteratively enrich encoder families through function composition. These results, as well as recent work [Das et al., 2020] on the properties of random deep neural networks, motivate us to approximate the optimal family of encoding functions as deep neural networks. While our theoretical results do not guarantee the security of our specific *NeuraCrypt* network architecture, we provide empirical experiments to test the robustness of our approach against modern attacks, following standard practice in cryptanalysis [Standard, 2001, Dworkin, 2015].

We empirically test our method on two benchmark chest x-ray datasets MIMIC-CXR [Johnson et al., 2019] and CheXpert [Irvin et al., 2019], and compare it against the model operating on raw data. We demonstrate that, across a variety of diagnostic tasks, *NeuraCrypt*-based models achieve competitive performance. Moreover, we show that combining multiple datasets, using separate private encoders, enables the model to benefit from additional training data and thereby improve its accuracy. *NeuraCrypt* appears robust to adversarial attacks designed to either uncover the private encoder or to uncover additional sensitive attributes from the encoded data.

We believe our *NeuraCrypt* architecture, as well as the core idea of using random deep neural network encodings to achieve privacy, provide a novel direction for privacy-preserving machine learning. We encourage the development of new attacks on *NeuraCrypt* as well as further refinements of our method, and to this end, we release a challenge dataset.

2 Related Work

Cryptographic techniques. Cryptographic techniques, such as secure multiparty computation and fully homomorphic encryption [Yao, 1986, Goldreich et al., 1987, Ben-Or et al., 1988, Chaum et al., 1988, Gentry, 2009, Brakerski and Vaikuntanathan, 2014, Cho et al., 2018], allow one or more data owners, such as hospitals, to encode (encrypt) their data before providing them to a third party, say a cloud data center, for computation. Building models with homomorphic encryption requires leveraging specialized cryptographic primitives, an approach that requires an impractical overhead for modern deep learning models. In contrast, *NeuraCrypt* encodings can be directly leveraged by standard deep learning techniques.

The high complexity of constructing and running homomorphic encryption generally provide extremely strong guarantees, such as a semantic security [Goldwasser and Micali, 1982], wherein no information regarding the original data may be leaked by the encoding or computation. However, this strong security guarantee is an overkill for our context. For instance, we do not seek to hide the fact that a hospital hosts chest x-rays or the disease labels of those x-rays, as we release the labels publicly. Our goal is to avoid expending design and run-time resources [Mohassel and Zhang, 2017, Liu et al., 2017, Juvekar et al., 2018, Bourse et al., 2018] on hiding these facts through homomorphic encryption. Rather, we seek to provide privacy by protecting the characteristics of a chest x-ray not already captured by the disease label.

Federated learning and differential privacy techniques. Federated learning (FL) [McMahan et al., 2017] enables collaborative learning among different data-owners (hospitals) through distributed training. The core idea of FL is to avoid transferring raw data by allocating an instance of the ML model at each data owner, and instead sharing model updates [Rieke et al., 2020]. Despite a considerable amount of research in this area, including progress in secure aggregation [Bonawitz et al., 2017] and differential privacy [Dwork et al., 2014], preserving privacy while maintaining modeling accuracy in FL remains an open challenge [Schoon, 2021, McMahan et al., 2021]. In contrast to *NeuraCrypt*, FL is not designed to enable data-owners to publicly deposit their data.

Lightweight encoding techniques. Our approach is most closely related to prior focused on achieving privacy through lightweight encoding schemes. [Ko et al., 2020, Tanaka, 2018, Sirichotedumrong et al., 2019] have proposed de-identification techniques to carefully distort images to reduce their recognition rate by humans while preserving the accuracy of image classification models. Unfortunately, such methods do not offer privacy against realistic attacks. Recently, InstaHide [Huang et al., 2020] proposed to encode images by linearly mixing them with other samples and applying a pixel-wise mask. While this approach provides collaborative learning for multiple data owners, its linear transforms preserve the relative distance between two samples in the original domain and the encoded domain. This drawback was exploited by [Carlini et al., 2021] to decrypt the Instahide dataset challenge. DAUnTLess [Xiao and Devadas, 2021] proposed to encode images using fully-connected neural networks and linear sample mixing, and analyzed the computational difficulty of reversing this encoding to an attacker with access to parallel raw and encoded data pairs. They demonstrate that this encoding is easy to reverse if the source data distribution has low entropy (e.g. MNIST), and more difficult for complex datasets. Moreover, they demonstrate that mixing samples can increase the difficulty of the recovery task. In contrast to DAUnTLess, we consider a threat model where the adversary is computationally-unbounded and does not have access to parallel data.

3 Method

NeuraCrypt. The problem setting is depicted in Figure 1. We wish to enable a hospital to publish their image dataset X_d with diagnostic labels Y_d while protecting patient privacy. Given the dataset $\{(x, y)\}_{x \in X_d}$, where $y = L(x)$ is the label, a data-owner randomly samples a private *NeuraCrypt* encoder T_d , a random neural network, and uses T_d to produce encoded samples $Z_d = T_d(X_d)$, i.e., $z_i = T_d(x_i)$ for every $x_i \in X_d$. The data-owner can then deposit $\{(T_d(x_i), L(x_i))\}_{x_i \in X_d}$ publicly for untrusted third parties to develop models to estimate $\Pr[Y_d = Y_d | Z_d = Z_d]$. We note that multiple data owners can seamlessly collaborate to develop joint models by publishing datasets on the same task while using independent *NeuraCrypt* encoders. Given that model developers can only estimate $\Pr[Y_d = Y_d | Z_d = Z_d]$ and not $\Pr[Y_d = Y_d | X_d = X_d]$, only data-owners can directly

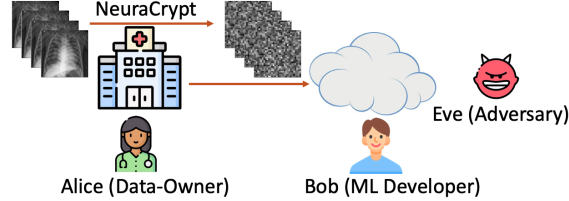


Figure 1: Alice (data-owner) transmits her labeled encoded data to Bob (ML developer). Eve (adversary) attempts to identify information about Alice’s raw data beyond their labels.

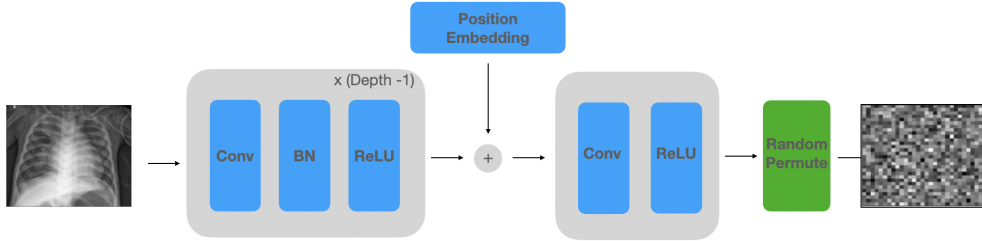


Figure 2: Architecture of *NeuraCrypt* encoder.

utilize the learned models, creating an incentive for data-owners and model developers to collaborate for model dissemination.

While many *NeuraCrypt* architectures are possible, we focus on medical imaging tasks, and thus implement our *NeuraCrypt* encoders as convolutional neural networks. Our encoder architecture is illustrated in Figure 2, and consists of convolutional layers with non-overlapping strides, batch normalization [Ioffe and Szegedy, 2015], and ReLU non-linearities. To encode positional information into the feature space while hiding spatial structure, we add a random positional embedding for each patch before the final convolutional and ReLU layers and randomly permute the patches at the output independently for each private sample. This results in an unordered set of patch feature vectors for each image. We note that this architecture is closely inspired by the design of patch-embedding modules in Vision Transformer networks [Dosovitskiy et al., 2020, Zhou et al., 2021].

Threat model. We assume a computationally unbounded adversary which knows all possible images \mathcal{X} as well as their labels, i.e., $\{(x, L(x))\}_{x \in \mathcal{X}}$. The adversary also knows the distributions of both the data-owners’ samples $\Pr[\mathbf{X}_d = X_d]$ and the choice of encoder function $\Pr[\mathbf{T}_d = T]$. This adversary knows $\{(T_d(x), L(x))\}_{x \in X_d}$, as the data owner deposits it publicly. Moreover, since we do not know the adversary’s classifying capabilities, we assume the worst case, in which she is able to perfectly classify the encoded samples. Thus, we assume the adversary also knows $\{(T_d(x), L(x))\}_{x \in \mathcal{X}}$, where now the images are taken over the whole of \mathcal{X} . The goal of the adversary is to learn more about the random variable \mathbf{X}_d using Z_d, Y_d than from Y_d alone. We define this formally in section 4.

Privacy intuition. We provide a formal privacy analysis for the described threat model given an encoder space \mathcal{F} in Section 4. We consider a theoretical \mathcal{F} which consists of all bijections from \mathcal{X} to \mathcal{X} with the same label assignment. These encodings map each image of the hospital’s dataset to another image in \mathcal{X} with the same label. This function family is exponentially large in size of \mathcal{X} and a computationally unbounded adversary, as described in our threat model, cannot distinguish between its members. In this setting, observing (Z_d, Y_d) does not offer the adversary more information about the underlying \mathbf{X}_d than observing Y_d . While sampling from this optimal family directly is not feasible, as it would require full knowledge of \mathcal{X} and its labels, our theoretical analysis demonstrates that we can enrich the privacy of our encoding scheme via functional composition. This result motivates us to approximate the \mathcal{F} using deep neural networks.

4 Privacy Analysis

In this section, we present a detailed analysis of the threat model in Section 3. All proofs appear in the appendix. We denote the set of all samples by \mathcal{X} and assume it is a finite set. Each sample $x \in \mathcal{X}$ is labeled by a function $L : \mathcal{X} \rightarrow \mathcal{Y}$, where the set of labels \mathcal{Y} is also finite. We denote the set of all bijections from \mathcal{X} to itself by $\text{Sym}(\mathcal{X}) = \{T : \mathcal{X} \rightarrow \mathcal{X} : T \text{ is a bijection}\}$. As each data-owner acts independently, we perform our analysis individually. We consider a model with three participants, Alice, Bob and Eve, to be consistent with the common terminology of privacy (see also Figure 1):

Alice (the data owner). Alice has a private subset of samples $X_A \subseteq \mathcal{X}$ which is drawn from a distribution $\Pr[\mathbf{X}_A = X_A]$. The subscript A for Alice replaces the generic subscript d used for X in our Method discussion. Alice samples an encoder T_A from a family $\mathcal{F} \subseteq \text{Sym}(\mathcal{X})$ according to a distribution $\Pr[\mathbf{T}_A = T]$, and then transmits $M_A(X_A) = \{(T_A(x), L(x))\}_{x \in X_A}$ to Bob. Alice does not know or have control over $\Pr[\mathbf{X}_A = X_A]$ but gets to choose \mathcal{F} and the distribution $\Pr[\mathbf{T}_A = T]$.

Bob (the model developer). Bob, who is not aware of the true labeling $L \in \mathcal{Y}^{\mathcal{X}}$, knows a prior distribution $\Pr[L = L']$, and also the distribution $\Pr[\mathbf{T}_A = T]$. After receiving $M_A(X_A) = \{(T_A(x), L(x))\}_{x \in X_A}$, he is interested in learning a classifier on Alice's encoded data, $L_A = L \circ T_A^{-1}$, i.e., the distribution $\Pr[L_A = L_A' \mid \mathbf{M}_A(\mathbf{X}_A) = M_A(X_A)]$, for every $x \in \mathcal{X}$.

Eve (the adversary). Eve knows $\{(x, L(x))\}_{x \in \mathcal{X}}$ and the distributions $\Pr[\mathbf{X}_A = X_A]$ and $\Pr[\mathbf{T}_A = T]$. Since Alice (e.g a hospital) releases the data publicly, Eve also knows $M_A(X_A) = \{(T_A(x), L(x))\}_{x \in X_A}$. While impractical, we consider a worst case scenario where Eve is able to classify perfectly any sample and thus, we also assume that she knows $M_A(\mathcal{X}) = \{(T_A(x), L(x))\}_{x \in \mathcal{X}}$. Eve is interested in learning the random variable \mathbf{X}_A .

In our model we are interested in comparing what Eve learns of Alice's samples \mathbf{X}_A from the observation of $M_A(X_A)$ and $M_A(\mathcal{X})$ compared to only having observed $Y_A = \{L(x)\}_{x \in X_A}$. In this context, we say Alice's scheme is *perfectly private* if $\Pr[\mathbf{X}_A = X_A \mid \mathbf{M}_A(\mathbf{X}_A) = M_A(X_A), \mathbf{M}_A(\mathcal{X}) = M_A(\mathcal{X})] = \Pr[\mathbf{X}_A = X_A \mid \mathbf{Y}_A = Y_A]$. Since Alice can only choose \mathcal{F} and its distribution $\Pr[\mathbf{T}_A = T]$, we often refer to \mathcal{F} as Alice's scheme.

For notation purposes, we occasionally impose a total order \preceq on \mathcal{X} to represent it by a vector $(x_1, \dots, x_{|\mathcal{X}|})$ such that $x_i \preceq x_j$ if $i \leq j$. We then represent a transformation T by a vector with size $|\mathcal{X}|$ whose i -th element is $T(x_i)$.

Next we define the *label configuration (LC)* and the *LC-anonymity list*, as these notions capture Eve's uncertainty about Alice's private samples X_A .

Definition 1 (Label configuration). The original label configuration, denoted by $\text{LC}(\mathcal{X})$, is a vector of size $|\mathcal{X}|$ whose i -th elements is $L(x_i)$. The label configuration of an encoder T , denoted by $\text{LC}(T)$, is a permutation of $\text{LC}(\mathcal{X})$ according to T , i.e. the i -th element of $\text{LC}(T)$ is $L \circ T^{-1}(x_i)$.

Definition 2 (LC-anonymity list). Given a family of encoders \mathcal{F} , the LC-anonymity list of an encoder $T \in \mathcal{F}$ is defined as $\mathcal{F}_T = \{T' \in \mathcal{F} : \text{LC}(T') = \text{LC}(T)\}$.

The LC-anonymity lists partition \mathcal{F} into different equivalence classes (see Figure 3). We also note that under these new concepts, Eve's knowledge of $M_A(X_A) = \{(T_A(x), L(x))\}_{x \in X_A}$ and $M_A(\mathcal{X}) = \{(T_A(x), L(x))\}_{x \in \mathcal{X}}$ is equivalent to her knowing $T_A(X_A)$ and $\text{LC}(T_A)$.

Example 1. Let $\mathcal{X} = \{1, \dots, 16\}$ and, for representation purposes, consider the ordering $1 \preceq 2 \preceq \dots \preceq 16$. Let $\mathcal{Y} = \{-, +\}$, and $\mathcal{F} = \text{Sym}(\mathcal{X})$. Let the labeling L be such that $\text{LC}(\mathcal{X}) = (+ + - - + + - - - - - - - -)$. Assume that Alice chooses $T_A = (12, 2, 11, 4, 6, 8, 16, 15, 13, 7, 9, 5, 3, 14, 1, 10)$, and that her data is $X_A = \{2, 5, 7, 10, 15\}$. Thus, she sends $\{(2, +), (6, +), (16, -), (7, -), (1, -)\}$ to Bob. According to the threat model, Eve knows $\text{LC}(T_A) = (- + - - - + - + - - - + - - -)$. Although $|\mathcal{F}| = 16! = 2.1\text{e}13$, since Eve knows $\text{LC}(T_A)$, she can infer that Alice's encoder is in the smaller set \mathcal{F}_{T_A} with cardinality $4!12! = 1.1\text{e}10$. Thus, if Alice had chosen T_A uniformly at random from \mathcal{F} , then the probability of Eve guessing T_A correctly would be approximately $1\text{e}-10$. Eve, however, is interested in learning X_A . In this case, since T_A is uniform over all permutations, it can be shown that \mathcal{F} is perfectly private, i.e. Eve learns no more than she would by solely observing $Y_A = \{L(x)\}_{x \in X_A}$.

As illustrated in the example above, the scheme where Alice chooses T_A uniformly from $\text{Sym}(\mathcal{X})$ is perfectly private. This scheme, however, completely scrambles of the dataset, making Bob's learning

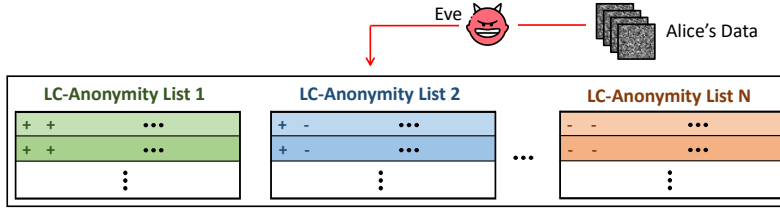


Figure 3: Eve receives Alice's encoded data and selects the correct set of encoders \mathcal{F}_{T_A} according to the observed label configuration. Eve cannot distinguish among encoders within one LC-anonymity list, and the best she can do is to identify the possible value for Alice's raw data corresponding to each encoder in the list.

task impossible. By observing a subset of the encoded data, Bob still cannot predict the label of a held-out sample better than the prior probability. In Theorem 2, we show that there exist schemes which are perfectly private, while still preserving the structure of X_A . Towards that, we begin by investigating the privacy of general families $\mathcal{F} \subseteq \text{Sym}(\mathcal{X})$.

We begin by characterizing the set of possible values for X_A , given Eve's observations.

Proposition 1. *The set of possible values for Alice's dataset, given Eve's observations, is*

$$\text{Pos}(X_A) \triangleq \{\bar{X} \in \mathcal{X}^{|X_A|} : \exists T \in \mathcal{F}_{T_A} \text{ with } T(\bar{X}) = T_A(X_A)\}.$$

The next theorem characterizes what Eve learns about X_A via Alice's scheme and what she would learn if, instead, she only observed $Y_A = \{L(x)\}_{x \in X_A}$.

Theorem 1. *Let X_A be the random variable for Alice's private samples and T_A be the random variable for Alice's encoder. We note $\mathbb{1}(\text{condition})$ is an indicator function which takes value one when condition happens and zero otherwise. Then,*

$$\Pr[X_A = X_A \mid T_A(X_A) = Z, \text{LC}(T_A) = C] \propto \sum_{\{T: \text{LC}(T)=C, T(X_A)=Z\}} \Pr[X_A = X_A] \Pr[T_A = T]$$

and

$$\Pr[X_A = X_A \mid Y_A = Y_A] \propto \mathbb{1}(Y_A = \{L(x)\}_{x \in X_A}) \cdot \Pr[X_A = X_A].$$

Since Theorem 1 fully characterizes how much Eve learns about Alice's private samples and the encoder T_A , any privacy metric, be it a mutual information [Shannon, 1948], a mean squared error, or a guessing measure [Pliam, 1999], can be computed from it.

The following example showcases the theorem.

Example 2. Let $\mathcal{X} = \{1, 2, 3, 4, 5\}$, $X_A = \{2, 3, 4\}$, $\text{LC}(\mathcal{X}) = (+ + - - -)$, and $\mathcal{F} = \{T_1, \dots, T_6\}$ given below. Suppose $T_A = T_1$. Then, Alice transmits $\{(1, +), (4, -), (5, -)\}$. Eve knows $\text{LC}(T_A) = (+ + - - -)$, and thus knows \mathcal{F}_{T_A} as well:

$$\mathcal{F} = \begin{cases} T_1 : (2, 1, 5, 4, 3) \\ T_2 : (2, 1, 3, 5, 4) \\ T_3 : (1, 2, 3, 5, 4) \\ T_4 : (4, 3, 1, 2, 5) \\ T_5 : (3, 4, 2, 1, 5) \\ T_6 : (5, 2, 4, 3, 1) \end{cases}, \quad \mathcal{F}_{T_A} = \begin{cases} T_1 : (2, 1, 5, 4, 3) \\ T_2 : (2, 1, 3, 5, 4) \\ T_3 : (1, 2, 3, 5, 4) \end{cases}.$$

As a result, $\text{Pos}(X_A) = \{(2, 4, 3), (2, 5, 4), (1, 5, 4)\}$. Thus, Eve knows that $4 \in X_A$ independent of the distribution of X_A . If we assume uniform distributions for T_A and X_A , then, by Theorem 1, we obtain a uniform distribution on $\text{Pos}(X_A)$ and can compute $\Pr[1 \in X_A] = 1/3$ and $\Pr[2 \in X_A] = 2/3$. If instead we assume uniform T_A and $\Pr[X_A = \{2, 3, 4\}] = 0.1$, $\Pr[X_A = \{2, 5, 4\}] = 0.1$, and $\Pr[X_A = \{1, 5, 4\}] = 0.4$, then $\Pr[1 \in X_A] = 2/3$ and $\Pr[2 \in X_A] = 1/3$. A more detailed version of this example is given in the appendix.

We now describe a scheme which achieves perfect privacy without affecting learnability.

Theorem 2. Let $\mathcal{X}^y = \{x \in \mathcal{X} : L(x) = y\}$. Then, sampling T_A uniformly from the family $\mathcal{F}_0 = \{T \in \text{Sym}(\mathcal{X}) : T(\mathcal{X}^y) = \mathcal{X}^y \ \forall y \in \mathcal{Y}\}$ achieves perfect privacy without altering the structure of the labels.

Although Theorem 2 shows the existence of an optimal family of encoders, Alice has no way of sampling from it as it would require full knowledge of \mathcal{X} and its labels. Thus, the theorem serves as a guide on what properties Alice might want from the family of encoders \mathcal{F} .

Starting from an imperfect \mathcal{F} , we now wish to understand what kind of operations Alice can perform to enrich the privacy of \mathcal{F} . To this end, we explore several ways to grow \mathcal{F} . In our next proposition, we show that adding arbitrary functions to \mathcal{F} might actually worsen the privacy.

Proposition 2. Let $\mathcal{F}, \mathcal{F}' \subseteq \text{Sym}(\mathcal{X})$ be two families of encoders such that $\mathcal{F} \subseteq \mathcal{F}'$. Then, it is not generally true that \mathcal{F}' is more private than \mathcal{F} .

However, as we now show, composing families of functions can only preserve or increase the privacy of the family.

Theorem 3. Let $\mathcal{F}, \mathcal{F}' \subseteq \text{Sym}(\mathcal{X})$ and $\mathcal{F}' \circ \mathcal{F} = \{T' \circ T : T' \in \mathcal{F}', T \in \mathcal{F}\}$. Then, $\mathcal{F}' \circ \mathcal{F}$ is no less private than \mathcal{F} .

Theorem 3 shows that composing families of encoders cannot reduce the privacy. Indeed, as we show in the following example, it can potentially increase it.

Example 3. Let $\mathcal{X} = \{1, 2, 3, 4, 5\}$ and $\text{LC}(\mathcal{X}) = (+ + - - -)$. The sets of encoders $\mathcal{F}, \mathcal{F}'$, and $\mathcal{F}' \circ \mathcal{F}$, along with the label configuration for each encoder, are given:

$$\mathcal{F} = \begin{cases} T_1 : (1, 2, 3, 4, 5), (+ + - - -) \\ T_2 : (2, 1, 3, 5, 4), (+ + - - -) \\ T_3 : (1, 2, 5, 4, 3), (+ + - - -) \\ T_4 : (1, 3, 2, 4, 5), (+ - + - -) \\ T_5 : (1, 5, 2, 3, 4), (+ - + - -) \end{cases} \quad \mathcal{F}' \circ \mathcal{F} = \begin{cases} T'_1 \circ T_1 : (1, 2, 3, 4, 5), (+ + - - -) \\ T'_1 \circ T_2 : (2, 1, 3, 5, 4), (+ + - - -) \\ T'_1 \circ T_3 : (1, 2, 5, 4, 3), (+ + - - -) \\ T'_1 \circ T_4 : (1, 3, 2, 4, 5), (+ - + - -) \\ T'_1 \circ T_5 : (1, 5, 2, 3, 4), (+ - + - -) \\ T'_2 \circ T_1 : (3, 2, 1, 4, 5), (- + + - -) \\ T'_2 \circ T_2 : (3, 1, 2, 5, 4), (- + + - -) \\ T'_2 \circ T_3 : (5, 2, 1, 4, 3), (- + + - -) \\ T'_2 \circ T_4 : (2, 3, 1, 4, 5), (+ - + - -) \\ T'_2 \circ T_5 : (2, 5, 1, 3, 4), (+ - + - -) \end{cases}$$

Here, \mathcal{F} has two LC-anonymity lists, with cardinality 2 and 3, and $\mathcal{F}' \circ \mathcal{F}$ has three LC-anonymity lists with cardinality 3, 3, and 4. Thus, it offers more ambiguity (better privacy) as its LC-anonymity lists have higher minimum cardinality compared to \mathcal{F} alone.

While we cannot directly sample from the optimal family of encoders, we can leverage our theoretical results on function composition to guide the design of *NeuraCrypt*. Starting with a weak encoder, i.e a linear layer, we iteratively enrich the privacy of our function family through function composition (e.g by adding with additional non-linear and linear layers), to build a random neural network. Moreover, given that we know that the labeling function L_A on medical images is likely to be efficiently estimated with a convolutional neural network, we implement our *NeuraCrypt* encoders as convolutional neural networks. We emphasize that our privacy guarantees for the optimal family do not extend to our implementation of *NeuraCrypt*, and thus its privacy must be tested empirically, following standard practice in cryptanalysis [Standard, 2001, Dworkin, 2015].

5 Experiments

Datasets. For all experiments, we utilized two benchmark datasets of chest x-rays, MIMIC-CXR (Johnson et al. [2019]) and CheXpert (Irvin et al. [2019]) from Beth Israel Deaconess Medical Center and Stanford respectively. For each dataset, we evaluated the ability of each model to predict Edema, Pneumothorax, Consolidation, Cardiomegaly and Atelectasis. For each task, we excluded exams with an uncertain disease label, i.e., the clinical diagnosis did not explicitly rule out or confirm the disease, and randomly split the remaining data 60–20–20 for training, development and testing respectively.

All images were down sampled to 256×256 pixels. All experiments were repeated 3 times across different seeds and we report each metric with its standard deviation.

5.1 Evaluating modeling utility

To evaluate the impact of *NeuraCrypt* encodings on downstream modeling performance, we compared *NeuraCrypt*-based models to standard architectures trained on raw images across both the single and multi-hospital setting. For each diagnosis task and training setting, we report the average AUC across the MIMIC-CXR and CheXpert test sets. We report results on the MIMIC-CXR and CheXpert datasets individually in the appendix. For *NeuraCrypt* multi-hospital training, we wished to evaluate the impact of leveraging independent *NeuraCrypt* encoders on modeling accuracy. As a result, we evaluate both model performance when leveraging a single encoder across both hospitals (Combined-Clear), and model performance when leveraging two independent encoders (Combined-Private). We note that performance in the Combined-Clear setting acts as an upper-bound for Combined-Private.

Our *NeuraCrypt* encoding leveraged a patch-size of 16×16 , a depth of 7, and a hidden dimension of 2048. This model had $\sim 22.9M$ parameters and mapped 256×256 pixel images to 256×2048 vectors. Due to the patch-shuffling step in *NeuraCrypt*, this representation is unordered. As a result, we trained Vision Transformers (ViT) [Zhou et al., 2021], a self-attention based architecture that is invariant to patch ordering. Across all experiments, we used a one-layer ViT with a hidden dimension of 2048. We compared *NeuraCrypt* model performance with a non-private baseline, namely an identical ViT model where the patch encoder is learned jointly. We trained all models for 25 epochs using the Adam optimizer [Kingma and Ba, 2014], an initial learning rate of $1e-04$, weight decay of $1e-03$ and a batch size of 128.

5.2 Evaluating robustness to attacks

Adversarial attack. To validate robustness of our encoding approach to attacks aimed at estimating T , we performed experiments on the combined MIMIC-CXR and CheXpert datasets with Cardiomegaly labels. We assumed that the attacker has access to the entire labeled dataset $\{(x_i, y_i)\}_{x_i \in X}$, and labeled *NeuraCrypt*-encoded samples $\{(z_i = T(x_i), y_i)\}_{x_i \in X}$. We also assumed that the attacker knows \mathcal{F} (the exact architecture of *NeuraCrypt*), but not the weights of T which are private. Given this information, the attacker tries to learn a T^* such that $T(X) \approx T^*(X)$. We assume that if T was leaked, the attacker could easily invert the encoding and recover the raw original images. To estimate T , we sampled an initial T^* with the same architecture as T , and trained it to minimize the accuracy of a domain discriminator, which aims to distinguish between the generated Z^* and true Z .

The discriminator is typically designed as a parameterized classifier [Tzeng et al., 2017, Goodfellow et al., 2014, Shen et al., 2017], and trained through a mini-max game with the encoder T^* . However, we found this difficult to train. Instead, we conducted experiments using Maximum Mean Discrepancy (MMD) [Gretton et al., 2012] as our discriminator. Specifically, we defined the MMD loss as for a batch of real ciphertext and generated ciphertext Z and Z^* as $L_{T^*} = \text{MMD}^2(Z, Z^*)$, where $\text{MMD}(Z, Z^*) = \|(\sum_z \phi(z))/|Z| - (\sum_{z^*} \phi(z^*))/|Z^*|\|_{\mathcal{H}}$ measures the discrepancy between Z and Z^* on a Reproducing Kernel Hilbert Space, and ϕ is a feature map induced by a linear combination of multiple RBF kernels $\kappa(z_i, z_j) = \sum_n \exp(-1/(2\sigma_n \|z_i - z_j\|^2))$. Our MMD formulation follows prior work in domain adaptation [Guo et al., 2018, Bousmalis et al., 2016].

In order to understand how the success of this attack would vary with the architecture of *NeuraCrypt*, we performed the attack on *NeuraCrypt* architectures with a depth of 2 and 7. As a baseline, we also performed the attack when using a simple linear encoder, implemented as single convolutional layer. Across all experiments, we used a hidden dimension of 2048 and trained T^* for 25 epochs. We performed a grid search over different learning rates and weight decay values for each attack. For each experiment, we evaluated the attack by measuring the mean squared error (MSE) between generated (Z^*) and real ciphertext (Z) for the same plaintext images across the dataset. To understand if T^* outperforms a trivial baseline, we compare the performance of T^* to the mean baseline T_μ , where $T_\mu(x) = \frac{1}{|Z|}(\sum_z z)$. T_μ ignores the input x and predicts the mean of Z for all inputs. We consider an attack to be successful if T^* outperforms T_μ , i.e., the ratio of $\frac{T^* \text{MSE}}{T_\mu \text{MSE}} < 1$. We consider additional experiments varying the architecture of T and T^* and provide additional analyses in the appendix.

Transfer learning attack. We also consider a scenario where an attacker may try to learn a sensitive attribute classifier, such as a gender predictor, on chest x-rays and tries to transfer this classifier onto the encoded data Z . If this transferred classifier performs better than random on Z , then an attacker, could leverage this approach to learn sensitive information not released by the data-owner or to propagate labels to be used in a refined adversarial attack. To validate the robustness of *NeuraCrypt* to this type of attack, we began with the best estimated T^* from our adversarial attack experiments, as measured by T^* MSE, and built a new classifier to predict Edema given Z^* . We report the ROC AUC of this classifier on both Z and Z^* . We performed these experiments on the combined MIMIC-CXR and CheXpert dataset. We performed this attack for both *NeuraCrypt*-encoding with a depth of 7 and a hidden dimension of 2048, as leveraged in the *modeling utility* experiments, and when using a linear encoding. For each experiment, we trained a ViT for 25 epochs using the Adam optimizer, an initial learning rate of $1e-04$ and a batch size of 128.

6 Results

Table 1: Impact of *NeuraCrypt* on chest x-ray prediction tasks across different training settings. All metrics are average ROC AUCs across the MIMIC-CXR and CheXpert test sets. Combined-Clear and Combined-Private refer to using a single *NeuraCrypt* encoder across the combined MIMIC-CXR and CheXpert datasets and two independent *NeuraCrypt* encoders respectively. Guides of abbreviations for medical diagnosis: (E)dema, (P)neumothorax, (Co)nsolidation, (Ca)rdiomegaly and (A)telectasis.

<i>Model</i>	E	P	Co	Ca	A	<i>Average</i>
Train on MIMIC-CXR						
ViT	85 ± 1	69 ± 3	74 ± 2	87 ± 0	83 ± 1	80
<i>NeuraCrypt</i> -ViT	85 ± 2	72 ± 1	72 ± 1	87 ± 0	83 ± 1	80
Train on CheXpert						
ViT	82 ± 1	71 ± 1	72 ± 3	83 ± 1	80 ± 0	77
<i>NeuraCrypt</i> -ViT	84 ± 1	71 ± 1	75 ± 2	82 ± 1	81 ± 0	79
Train on Combined-Clear						
ViT	86 ± 0	77 ± 1	76 ± 2	87 ± 1	85 ± 0	82
<i>NeuraCrypt</i> -ViT	87 ± 0	76 ± 3	78 ± 1	88 ± 0	85 ± 1	83
Train on Combined-Private						
<i>NeuraCrypt</i> -ViT	87 ± 1	77 ± 3	77 ± 3	86 ± 1	84 ± 1	82

Evaluating modeling utility. We report our results in predicting various medical diagnoses from chest x-ray datasets in Table 1. *NeuraCrypt*-ViT obtained competitive AUCs to our non-private ViT baseline across all training settings. In the multi-hospital setting, we found that *NeuraCrypt*-ViT was effectively able to leverage the larger training set to learn an improved classifier, despite using separate encoders for each dataset. *NeuraCrypt*-ViT obtained an average AUC increase of 2 and 3 points compared to training only on the MIMIC-CXR and CheXpert datasets respectively. Moreover, *NeuraCrypt* demonstrated achieved equivalent performance in the Combined-Clear and Combined-Private settings, demonstrating that multiple institutions do not pay a significant performance cost to collaborate privately.

Table 2: Left: MSE of MMD-based adversarial attacks on different *NeuraCrypt* encodings. T_μ refers to the mean baseline, and T^* refers to the encoder learned via the MMD attack. Right: Performance of transfer learning attack on Linear and *NeuraCrypt* encodings.

Encoding	$T^* \text{MSE} / T_\mu \text{MSE}$	Encoding	$T^* \text{AUC}$	$T \text{AUC}$
Linear	0.43 ± 0.01	Linear	89 ± 1	86 ± 1
<i>NeuraCrypt</i> -depth-2	7.97 ± 0.28	<i>NeuraCrypt</i>	84 ± 1	52 ± 4
<i>NeuraCrypt</i> -depth-7	4.44 ± 0.12			

Evaluating robustness to attacks. We report the performance of our adversarial and transfer learning attacks in Table 2 left and right panels respectively. As expected, using a linear encoding is not robust to either adversarial or transfer learning based attacks. We found that the adversarial attack outperformed the mean baseline (i.e. $\frac{T^* \text{MSE}}{T_\mu \text{MSE}} < 1$), and an Edema classifier trained on T^* transferred well to T encodings. In contrast, our adversarial attack on *NeuraCrypt* failed to outperform the mean

baseline when both using 2 and 7 layers. Moreover, *NeuraCrypt* was robust to our transfer learning attack, with the Edema classifier failing to obtain a AUC significantly better than random on the true T encodings.

7 Conclusion

We proposed *NeuraCrypt*, a private encoding scheme based on random neural networks designed to enable data owners to publicly publish their datasets while retaining data privacy and modeling utility. On two benchmark chest x-ray datasets, MIMIC-CXR and CheXpert, we found that *NeuraCrypt*-models obtained competitive performance to our non-private baselines. In the multi-institutional setting, where each site leverages an independent name encoder, we demonstrated that *NeuraCrypt*-models could effectively leverage the larger training data to learn improved classifiers. While this paper focused on medical imaging and chest X-ray tasks, *NeuraCrypt* can easily be extended to new data modalities such as text or molecular graphs. While we are not able to sample from the optimal family of encoders identified in our theoretical analysis, our analysis also provided a useful guide (i.e. function composition) for the design of *NeuraCrypt*. Similar to prior work in cryptanalysis [Standard, 2001, Dworkin, 2015], we note that our empirical results on adversarial robustness are not sufficient to prove the privacy of our architecture family for *NeuraCrypt*. Improved algorithms for domain adaption [Tzeng et al., 2017, Guo et al., 2018] or unsupervised translation [Lample et al., 2017, Alvarez-Melis and Jaakkola, 2018] specialized to the design of *NeuraCrypt* may yield more successful attacks. We release a challenge dataset to both encourage the development of new attacks on *NeuraCrypt* as well as the development of improved *NeuraCrypt* architectures.

References

- David Alvarez-Melis and Tommi S Jaakkola. Gromov-wasserstein alignment of word embedding spaces. *arXiv preprint arXiv:1809.00013*, 2018. pages 10
- Michael Ben-Or, Shafi Goldwasser, and Avi Wigderson. Completeness theorems for non-cryptographic fault-tolerant distributed computation (extended abstract). In Janos Simon, editor, *Proceedings of the 20th Annual ACM Symposium on Theory of Computing, May 2-4, 1988, Chicago, Illinois, USA*, pages 1–10. ACM, 1988. pages 3
- Keith Bonawitz, Vladimir Ivanov, Ben Kreuter, Antonio Marcedone, H Brendan McMahan, Sarvar Patel, Daniel Ramage, Aaron Segal, and Karn Seth. Practical secure aggregation for privacy-preserving machine learning. In *proceedings of the 2017 ACM SIGSAC Conference on Computer and Communications Security*, pages 1175–1191, 2017. pages 3
- Dan Boneh, Amit Sahai, and Brent Waters. Functional encryption: a new vision for public-key cryptography. *Commun. ACM*, 55(11):56–64, 2012. doi: 10.1145/2366316.2366333. URL <https://doi.org/10.1145/2366316.2366333>. pages 2
- Florian Bourse, Michele Minelli, Matthias Minihold, and Pascal Paillier. Fast homomorphic evaluation of deep discretized neural networks. In *Advances in Cryptology*, volume 10993, pages 483–512. Springer, 2018. pages 3
- Konstantinos Bousmalis, George Trigeorgis, Nathan Silberman, Dilip Krishnan, and Dumitru Erhan. Domain separation networks. *arXiv preprint arXiv:1608.06019*, 2016. pages 8
- Zvika Brakerski and Vinod Vaikuntanathan. Efficient fully homomorphic encryption from (standard) LWE. In Rafail Ostrovsky, editor, *IEEE 52nd Annual Symposium on Foundations of Computer Science, FOCS 2011, Palm Springs, CA, USA, October 22-25, 2011*, pages 97–106. IEEE Computer Society, 2011. doi: 10.1109/FOCS.2011.12. URL <https://doi.org/10.1109/FOCS.2011.12>. pages 2
- Zvika Brakerski and Vinod Vaikuntanathan. Efficient fully homomorphic encryption from (standard) LWE. *SIAM J. Comput.*, 43(2):831–871, 2014. doi: 10.1137/120868669. URL <https://doi.org/10.1137/120868669>. pages 3
- Nicholas Carlini, Samuel Deng, Sanjam Garg, Somesh Jha, Saeed Mahloujifar, Mohammad Mahmoudy, Shuang Song, Abhradeep Thakurta, and Florian Tramèr. Is private learning possible with instance encoding?, 2021. pages 3

- David Chaum, Claude Crépeau, and Ivan Damgård. Multiparty unconditionally secure protocols (extended abstract). In Janos Simon, editor, *Proceedings of the 20th Annual ACM Symposium on Theory of Computing, May 2-4, 1988, Chicago, Illinois, USA*, pages 11–19. ACM, 1988. pages 3
- Hyunghoon Cho, David J Wu, and Bonnie Berger. Secure genome-wide association analysis using multiparty computation. *Nature biotechnology*, 36(6):547–551, 2018. pages 2, 3
- Abhimanyu Das, Sreenivas Gollapudi, Ravi Kumar, and Rina Panigrahy. On the learnability of random deep networks. In Shuchi Chawla, editor, *Proceedings of the 2020 ACM-SIAM Symposium on Discrete Algorithms, SODA 2020, Salt Lake City, UT, USA, January 5-8, 2020*, pages 398–410. SIAM, 2020. doi: 10.1137/1.9781611975994.24. URL <https://doi.org/10.1137/1.9781611975994.24>. pages 2
- Alexey Dosovitskiy, Lucas Beyer, Alexander Kolesnikov, Dirk Weissenborn, Xiaohua Zhai, Thomas Unterthiner, Mostafa Dehghani, Matthias Minderer, Georg Heigold, Sylvain Gelly, et al. An image is worth 16x16 words: Transformers for image recognition at scale. *arXiv preprint arXiv:2010.11929*, 2020. pages 4
- Cynthia Dwork, Aaron Roth, et al. The algorithmic foundations of differential privacy. *Foundations and Trends in Theoretical Computer Science*, 9(3-4):211–407, 2014. pages 3
- Morris J Dworkin. SHA-3 standard: Permutation-based hash and extendable-output functions. 2015. pages 2, 7, 10
- GDPR. *EU General Data Protection Regulation of 2016*. pages 2
- Craig Gentry. Fully homomorphic encryption using ideal lattices. In Michael Mitzenmacher, editor, *Proceedings of the 41st Annual ACM Symposium on Theory of Computing, STOC 2009, Bethesda, MD, USA, May 31 - June 2, 2009*, pages 169–178. ACM, 2009. doi: 10.1145/1536414.1536440. URL <https://doi.org/10.1145/1536414.1536440>. pages 2, 3
- Oded Goldreich, Silvio Micali, and Avi Wigderson. How to play any mental game or A completeness theorem for protocols with honest majority. In Alfred V. Aho, editor, *Proceedings of the 19th Annual ACM Symposium on Theory of Computing, 1987, New York, New York, USA*, pages 218–229. ACM, 1987. pages 3
- Shafi Goldwasser and Silvio Micali. Probabilistic encryption and how to play mental poker keeping secret all partial information. In Harry R. Lewis, Barbara B. Simons, Walter A. Burkhard, and Lawrence H. Landweber, editors, *Proceedings of the 14th Annual ACM Symposium on Theory of Computing, May 5-7, 1982, San Francisco, California, USA*, pages 365–377. ACM, 1982. pages 3
- Ian J Goodfellow, Jean Pouget-Abadie, Mehdi Mirza, Bing Xu, David Warde-Farley, Sherjil Ozair, Aaron Courville, and Yoshua Bengio. Generative adversarial networks. *arXiv preprint arXiv:1406.2661*, 2014. pages 8
- Arthur Gretton, Karsten M Borgwardt, Malte J Rasch, Bernhard Schölkopf, and Alexander Smola. A kernel two-sample test. *The Journal of Machine Learning Research*, 13(1):723–773, 2012. pages 8
- Jiang Guo, Darsh J Shah, and Regina Barzilay. Multi-source domain adaptation with mixture of experts. *arXiv preprint arXiv:1809.02256*, 2018. pages 8, 10
- HIPAA. *Health Insurance Portability and Accountability Act of 1996*. pages 2
- Yangsibo Huang, Zhao Song, Kai Li, and Sanjeev Arora. InstaHide: Instance-hiding schemes for private distributed learning. In Hal Daumé III and Aarti Singh, editors, *Proceedings of the 37th International Conference on Machine Learning*, volume 119 of *Proceedings of Machine Learning Research*, pages 4507–4518. PMLR, 13–18 Jul 2020. pages 3
- Sergey Ioffe and Christian Szegedy. Batch normalization: Accelerating deep network training by reducing internal covariate shift. In *International conference on machine learning*, pages 448–456. PMLR, 2015. pages 4

- Jeremy Irvin, Pranav Rajpurkar, Michael Ko, Yifan Yu, Silvana Ciurea-Ilcus, Chris Chute, Henrik Marklund, Behzad Haghgoo, Robyn Ball, Katie Shpanskaya, et al. Chexpert: A large chest radiograph dataset with uncertainty labels and expert comparison. In *Proceedings of the AAAI Conference on Artificial Intelligence*, volume 33, pages 590–597, 2019. pages 2, 7
- Alistair EW Johnson, Tom J Pollard, Nathaniel R Greenbaum, Matthew P Lungren, Chih-ying Deng, Yifan Peng, Zhiyong Lu, Roger G Mark, Seth J Berkowitz, and Steven Horng. Mimic-cxr-jpg, a large publicly available database of labeled chest radiographs. *arXiv preprint arXiv:1901.07042*, 2019. pages 2, 7
- Chiraag Juvekar, Vinod Vaikuntanathan, and Anantha Chandrakasan. Gazelle: A low latency framework for secure neural network inference. In *Proceedings of the 27th USENIX Conference on Security Symposium, SEC'18*, page 1651–1668, USA, 2018. USENIX Association. ISBN 9781931971461. pages 3
- Diederik P Kingma and Jimmy Ba. Adam: A method for stochastic optimization. *arXiv preprint arXiv:1412.6980*, 2014. pages 8
- D. Ko, S. Choi, J. Shin, P. Liu, and Y. Choi. Structural image De-Identification for privacy-Preserving deep learning. *IEEE Access*, 8:119848–119862, 2020. pages 3
- Guillaume Lample, Alexis Conneau, Ludovic Denoyer, and Marc’Aurelio Ranzato. Unsupervised machine translation using monolingual corpora only. *arXiv preprint arXiv:1711.00043*, 2017. pages 10
- Jian Liu, Mika Juuti, Yao Lu, and N. Asokan. Oblivious neural network predictions via minionn transformations. In *Proceedings of the 2017 ACM SIGSAC Conference on Computer and Communications Security, CCS '17*, page 619–631, New York, NY, USA, 2017. Association for Computing Machinery. ISBN 9781450349468. doi: 10.1145/3133956.3134056. URL <https://doi.org/10.1145/3133956.3134056>. pages 3
- Brendan McMahan, Eider Moore, Daniel Ramage, Seth Hampson, and Blaise Aguera y Arcas. Communication-efficient learning of deep networks from decentralized data. In *Artificial Intelligence and Statistics*, pages 1273–1282. PMLR, 2017. pages 2, 3
- H Brendan McMahan et al. Advances and open problems in federated learning. *Foundations and Trends® in Machine Learning*, 14(1), 2021. pages 3
- Payman Mohassel and Yupeng Zhang. Secureml: A system for scalable privacy-preserving machine learning. In *2017 IEEE Symposium on Security and Privacy, SP 2017, San Jose, CA, USA, May 22-26, 2017*, pages 19–38. IEEE Computer Society, 2017. doi: 10.1109/SP.2017.12. URL <https://doi.org/10.1109/SP.2017.12>. pages 3
- John O Pliam. Guesswork and variation distance as measures of cipher security. In *International Workshop on Selected Areas in Cryptography*, pages 62–77. Springer, 1999. pages 6
- Nicola Rieke, Jonny Hancox, Wenqi Li, Fausto Milletari, Holger R. Roth, Shadi Albarqouni, Spyridon Bakas, Mathieu N. Galtier, Bennett A. Landman, Klaus Maier-Hein, Sébastien Ourselin, Micah Sheller, Ronald M. Summers, Andrew Trask, Daguang Xu, Maximilian Baust, and M. Jorge Cardoso. The future of digital health with federated learning. *npj Digital Medicine*, 3(1):119, 2020. URL <https://doi.org/10.1038/s41746-020-00323-1>. pages 3
- Ben Schoon. *Now EU regulators are worried about Google’s FLoC initiative, too (last accessed May 2021)*, 2021. URL <https://9to5google.com/2021/04/30/google-floc-eu-regulators/>. pages 3
- Claude E. Shannon. A mathematical theory of communication. *Bell Syst. Tech. J.*, 27(3):379–423, 1948. pages 6
- Tianxiao Shen, Tao Lei, Regina Barzilay, and Tommi Jaakkola. Style transfer from non-parallel text by cross-alignment. *arXiv preprint arXiv:1705.09655*, 2017. pages 8

- W. Sirichotedumrong, T. Maekawa, Y. Kinoshita, and H. Kiya. Privacy-preserving deep neural networks with pixel-based image encryption considering data augmentation in the encrypted domain. In *IEEE International Conference on Image Processing (ICIP)*, pages 674–678, 2019. pages 3
- NIST-FIPS Standard. Announcing the advanced encryption standard (AES). *Federal Information Processing Standards Publication*, 197(1-51):3–3, 2001. pages 2, 7, 10
- M. Tanaka. Learnable image encryption. In *IEEE International Conference on Consumer Electronics-Taiwan (ICCE-TW)*, pages 1–2, 2018. pages 3
- Eric Tzeng, Judy Hoffman, Kate Saenko, and Trevor Darrell. Adversarial discriminative domain adaptation. In *Proceedings of the IEEE conference on computer vision and pattern recognition*, pages 7167–7176, 2017. pages 8, 10
- Hanshen Xiao and Srinivas Devadas. Dauntless: Data augmentation and uniform transformation for learning with scalability and security. *Cryptology ePrint Archive*, Report 2021/201, 2021. <https://eprint.iacr.org/2021/201>. pages 3
- Andrew Chi-Chih Yao. How to generate and exchange secrets (extended abstract). In *27th Annual Symposium on Foundations of Computer Science, Toronto, Canada, 27-29 October 1986*, pages 162–167. IEEE Computer Society, 1986. pages 3
- Daquan Zhou, Bingyi Kang, Xiaojie Jin, Linjie Yang, Xiaochen Lian, Zihang Jiang, Qibin Hou, and Jiashi Feng. Deepvit: Towards deeper vision transformer. *arXiv preprint arXiv:2103.11886*, 2021. pages 4, 8

A Broader impact

Our study proposes a method to enable data-owners, e.g hospitals, to share their data publicly while protecting both patient privacy and modeling utility. We hope that this technology will enable the construction of diverse multi-center patient cohorts, and allow the broader machine learning community to contribute to the development of healthcare algorithms. We believe that improved algorithms in this space will lead to more equitable and precise healthcare. However, we acknowledge that the same privacy-preserving technology could be used to accelerate unethical biomedical research.

B Proofs of theoretical analysis

In this section, we prove the results of Section 4 and give an extended version of Example 2. We begin by proving the following lemma.

Lemma 1. *Let \mathbf{X}_A be the random variable for Alice’s private samples and \mathbf{T}_A be the random variable for Alice’s encoder. Then, $\Pr[\mathbf{X}_A = X_A, \mathbf{T}_A = T \mid \mathbf{T}_A(\mathbf{X}_A) = Z, \mathbf{LC}(\mathbf{T}_A) = C]$ is proportional to $\mathbb{1}(T(X_A) = Z) \cdot \mathbb{1}(\mathbf{LC}(T) = C) \cdot \Pr[\mathbf{X}_A = X_A] \cdot \Pr[\mathbf{T}_A = T]$.*

Proof of Lemma 1. Let $P_1 = \Pr[\mathbf{X}_A = X_A, \mathbf{T}_A = T \mid \mathbf{T}_A(\mathbf{X}_A) = Z, \mathbf{LC}(\mathbf{T}_A) = C]$ be the conditional joint distribution of \mathbf{X}_A and \mathbf{T}_A , $P_2 = \Pr[\mathbf{X}_A = X_A \mid \mathbf{T}_A = T, \mathbf{T}_A(\mathbf{X}_A) = Z, \mathbf{LC}(\mathbf{T}_A) = C]$, and $P_3 = \Pr[\mathbf{T}_A = T \mid \mathbf{T}_A(\mathbf{X}_A) = Z, \mathbf{LC}(\mathbf{T}_A) = C]$. Then, $P_1 = P_2 P_3$, and a direct calculation shows that $P_2 = \mathbb{1}(T(X_A) = Z)$. As for P_3 , it follows from Bayes’ theorem that

$$P_3 \propto \Pr[\mathbf{T}_A(\mathbf{X}_A) = Z \mid \mathbf{T}_A = T, \mathbf{LC}(\mathbf{T}_A) = C] \cdot \Pr[\mathbf{T}_A = T, \mathbf{LC}(\mathbf{T}_A) = C]. \quad (1)$$

Next, we have $\Pr[\mathbf{T}_A(\mathbf{X}_A) = Z \mid \mathbf{T}_A = T, \mathbf{LC}(\mathbf{T}_A) = C] = \Pr[\mathbf{X}_A = T^{-1}(Z)]$. Also, by Bayes’ theorem, $\Pr[\mathbf{T}_A = T, \mathbf{LC}(\mathbf{T}_A) = C] \propto \Pr[\mathbf{LC}(\mathbf{T}_A) = C \mid \mathbf{T}_A = T] \cdot \Pr[\mathbf{T}_A = T]$. Finally, from a direct calculation we obtain $\Pr[\mathbf{LC}(\mathbf{T}_A) = C \mid \mathbf{T}_A = T] = \mathbb{1}(\mathbf{LC}(T) = C)$. The result follows from substituting everything into (1) and multiplying by P_2 . We note that $\mathbb{1}(T(X_A) = Z) \cdot \Pr[\mathbf{X}_A = T^{-1}(Z)] = \mathbb{1}(T(X_A) = Z) \cdot \Pr[\mathbf{X}_A = X_A]$. \square

Theorem 1. Let \mathbf{X}_A be the random variable for Alice's private samples and \mathbf{T}_A be the random variable for Alice's encoder. Then,

$$\Pr[\mathbf{X}_A = X_A \mid \mathbf{T}_A(\mathbf{X}_A) = Z, \mathbf{LC}(\mathbf{T}_A) = C] \propto \sum_{\{T: \mathbf{LC}(T)=C, T(X_A)=Z\}} \Pr[\mathbf{X}_A = X_A] \Pr[\mathbf{T}_A = T]$$

and

$$\Pr[\mathbf{X}_A = X_A \mid \mathbf{Y}_A = Y_A] \propto \mathbb{1}(Y_A = \{L(x)\}_{x \in X_A}) \cdot \Pr[\mathbf{X}_A = X_A].$$

Proof of Theorem 1. For the first statement,

$$P_A = \sum_T \Pr[\mathbf{X}_A = X_A, \mathbf{T}_A = T \mid \mathbf{T}_A(\mathbf{X}_A) = Z, \mathbf{LC}(\mathbf{T}_A) = C] \quad (2)$$

$$\propto \sum_T \mathbb{1}(T(X_A) = Z) \cdot \mathbb{1}(\mathbf{LC}(T) = C) \cdot \Pr[\mathbf{X}_A = X_A] \cdot \Pr[\mathbf{T}_A = T] \quad (3)$$

$$= \sum_{\{T: \mathbf{LC}(T)=C, T(X_A)=Z\}} \Pr[\mathbf{X}_A = X_A] \cdot \Pr[\mathbf{T}_A = T], \quad (4)$$

where (2) follows from obtaining the marginal distribution from the joint distribution, and (3) follows from Lemma 1.

As for the second statement, from an application of Bayes' theorem, we obtain

$$\begin{aligned} \Pr[\mathbf{X}_A = X_A \mid \mathbf{Y}_A = Y_A] &\propto \Pr[\mathbf{Y}_A = Y_A \mid \mathbf{X}_A = X_A] \cdot \Pr[\mathbf{X}_A = X_A] \\ &\propto \mathbb{1}(Y_A = \{L(x)\}_{x \in X_A}) \cdot \Pr[\mathbf{X}_A = X_A]. \end{aligned}$$

□

Proposition 1. The set of possible values for Alice's dataset, given Eve's observations, is

$$\text{Pos}(X_A) \triangleq \{\bar{X} : \exists T \in \mathcal{F}_{T_A} \text{ with } T(\bar{X}) = T_A(X_A)\}.$$

Proof of Proposition 1. Let $Z = T_A(X_A)$, $C = \mathbf{LC}(T_A)$, and $X \notin \text{Pos}(X_A)$. Then, there does not exist a $T \in \mathcal{F}_A$ such that $T(X) = Z$. But $T \in \mathcal{F}_A$ if and only if $\mathbf{LC}(T) = C$. Thus, $\{T : \mathbf{LC}(T) = C, T(X) = Z\} = \emptyset$, and therefore, it follows from Theorem 1 that

$$\Pr[\mathbf{X}_A = X \mid \mathbf{T}_A(\mathbf{X}_A) = Z, \mathbf{LC}(\mathbf{T}_A) = C] = 0.$$

□

Extended version of Example 2. Let $\mathcal{X} = \{1, 2, 3, 4, 5\}$, $X_A = \{2, 3, 4\}$, $\mathbf{LC}(\mathcal{X}) = (++---)$, and

$$\mathcal{F} = \begin{cases} T_1 : (2, 1, 5, 4, 3) \\ T_2 : (2, 1, 3, 5, 4) \\ T_3 : (1, 2, 3, 5, 4) \\ T_4 : (4, 3, 1, 2, 5) \\ T_5 : (3, 4, 2, 1, 5) \\ T_6 : (5, 2, 4, 3, 1) \end{cases}.$$

- Suppose $T_A = T_1$. Then, Alice transmits $\{(1, +), (5, -), (4, -)\}$. Under our threat model, we assume that Eve knows $\mathbf{LC}(T_A) = (++---)$, and therefore, that T_A is in the set

$$\mathcal{F}_{T_A} = \begin{cases} T_1 : (2, 1, 5, 4, 3) \\ T_2 : (2, 1, 3, 5, 4) \\ T_3 : (1, 2, 3, 5, 4) \end{cases}.$$

which implies that $X_A \in \text{Pos}(X_A) = \{(2, 3, 4), (2, 4, 5), (1, 4, 5)\}$. Thus, Eve knows that $4 \in X_A$ independent of any distribution for X_A . As for the the two other values, it follows from Theorem 1 that

$$\begin{aligned} \Pr[1 \in \mathbf{X}_A] &= \sum_{\{\bar{X}: 1 \in \bar{X}\}} \Pr[\mathbf{X}_A = \bar{X} \mid \mathbf{T}_A(\mathbf{X}_A) = (1, 5, 4), \mathbf{LC}(\mathbf{T}_A) = (++---)] \\ &= \frac{\Pr[\mathbf{X}_A = (1, 4, 5)] \Pr[\mathbf{T}_A = T_3]}{\Pr[\mathbf{X}_A = (2, 3, 4)] \Pr[\mathbf{T}_A = T_1] + \Pr[\mathbf{X}_A = (2, 4, 5)] \Pr[\mathbf{T}_A = T_2] + \Pr[\mathbf{X}_A = (1, 4, 5)] \Pr[\mathbf{T}_A = T_3]} \end{aligned}$$

and

$$\begin{aligned} \Pr[2 \in \mathbf{X}_A] &= \sum_{\{x:2 \in x\}} \Pr[\mathbf{X}_A = \bar{x} \mid \mathbf{T}_A(\mathbf{X}_A) = (1, 5, 4), \mathbf{LC}(\mathbf{T}_A) = (+ + - - -)] \\ &= \frac{\Pr[\mathbf{X}_A = (2, 3, 4)] \Pr[\mathbf{T}_A = T_1] + \Pr[\mathbf{X}_A = (2, 4, 5)] \Pr[\mathbf{T}_A = T_2]}{\Pr[\mathbf{X}_A = (2, 3, 4)] \Pr[\mathbf{T}_A = T_1] + \Pr[\mathbf{X}_A = (2, 4, 5)] \Pr[\mathbf{T}_A = T_2] + \Pr[\mathbf{X}_A = (1, 4, 5)] \Pr[\mathbf{T}_A = T_3]} \end{aligned}$$

If we assume uniform distributions for T_A and uniform and iid distribution for samples in X_A , then $\Pr[1 \in X_A] = 1/3$ and $\Pr[2 \in X_A] = 2/3$. If we instead assume uniform T_A and that $\Pr[X_A = \{2, 3, 4\}] = 0.1$, $\Pr[X_A = \{2, 4, 5\}] = 0.1$, and $\Pr[X_A = \{1, 4, 5\}] = 0.4$, then $\Pr[1 \in X_A] = 2/3$ and $\Pr[2 \in X_A] = 1/3$.

- Suppose $T_A = T_4$. Then, Alice transmits $\{(3, +), (1, -), (2, -)\}$. Eve knows $\mathbf{LC}(T_A) = (- - + + -)$, and

$$\mathcal{F}_{T_A} = \begin{cases} T_4 : & (4, 3, 1, 2, 5) \\ T_5 : & (3, 4, 2, 1, 5) \end{cases}$$

and $\text{Pos}(X_A) = \{(2, 3, 4), (1, 4, 3)\}$. Thus, Eve knows that $\{3, 4\} \subset X_A$. The other probabilities can be derived in a similar way to the above item.

- Suppose $T_A = T_6$. Then, Alice transmits $\{(2, +), (4, -), (3, -)\}$. Eve knows $\mathbf{LC}(T_A) = (- + - - +)$, and

$$\mathcal{F}_{T_A} = \{T_6 : (5, 2, 4, 3, 1)\}$$

and, therefore, $\text{Pos}(X_A) = \{(2, 3, 4)\}$. In this case, Eve can exactly determine X_A .

Theorem 2. Let $\mathcal{X}^y = \{x \in \mathcal{X} : L(x) = y\}$. Then, sampling T_A uniformly from the family $\mathcal{F}_0 = \{T \in \text{Sym}(\mathcal{X}) : T(\mathcal{X}^y) = \mathcal{X}^y \ \forall y \in \mathcal{Y}\}$ achieves perfect privacy without altering the structure of the labels.

Proof of Theorem 2. Let $Z = T_A(X_A)$ and $C = \mathbf{LC}(T_A)$. We note that every $T \in \mathcal{F}_0$ has the same label configuration, i.e., $\mathbf{LC}(T) = \mathbf{LC}(\mathcal{X}) = C$. It follows then from Theorem 1 that

$$\begin{aligned} \Pr[\mathbf{X}_A = X \mid \mathbf{T}_A(\mathbf{X}_A) = Z, \mathbf{LC}(\mathbf{T}_A) = C] \\ &= \sum_{T \in \mathcal{F}_0} \mathbb{1}(T(X) = Z) \cdot \mathbb{1}(\mathbf{LC}(\mathcal{X}) = C) \cdot \Pr[\mathbf{X}_A = X] \cdot \Pr[\mathbf{T}_A = T] \\ &= \sum_{T \in \mathcal{F}_0} \mathbb{1}(T(X) = Z) \cdot \Pr[\mathbf{X}_A = X] \cdot \Pr[\mathbf{T}_A = T]. \end{aligned}$$

Since T is chosen uniformly from \mathcal{F}_0 , it follows that

$$\begin{aligned} \Pr[\mathbf{X}_A = X \mid \mathbf{T}_A(\mathbf{X}_A) = Z, \mathbf{LC}(\mathbf{T}_A) = C] \\ \propto \Pr[\mathbf{X}_A = X] \sum_{T \in \mathcal{F}_0} \mathbb{1}(T(X) = Z) = \Pr[\mathbf{X}_A = X] \cdot |\{T \in \mathcal{F}_0 : T(X) = Z\}|. \quad (5) \end{aligned}$$

Since Eve knows the set Z and the label configuration C , then she also knows the set of labels $Y_A = \{L(x)\}_{x \in X_A}$. The reason for this is that C is the vector representation of the labeling function $L \circ T^{-1}$, and thus, since Eve knows C and Z , she also knows $Y_A = L \circ T^{-1}(Z)$. We also note that the equality $\{L(x)\}_{x \in X} = Y_A$ holds if and only if the labels of X and Z are in agreement, i.e., $|\{x \in X : L(x) = y\}| = |\{z \in Z : L \circ T^{-1}(z) = y\}|$ for every $y \in \mathcal{Y}$. This is equivalent to the relation

$$\mathbb{1}(Y_A = \{L(x)\}_{x \in X}) = \prod_{y \in \mathcal{Y}} \mathbb{1}(|X^y| = |Z^y|),$$

where $X^y = \{x \in X : L(x) = y\}$ and $Z^y = \{z \in Z : L \circ T^{-1}(z) = y\}$.

On the other hand,

$$|\{T \in \mathcal{F}_0 : T(X) = Z\}| = \prod_{y \in \mathcal{Y}} |X^y|! \cdot \mathbb{1}(|X^y| = |Z^y|).$$

We note that $|X^y|$ does not depend on X and is in fact given by the number of elements with value y in Y_A . Thus,

$$|\{T \in \mathcal{F}_0 : T(X) = Z\}| \propto \prod_{y \in \mathcal{Y}} \mathbb{1}(|X^y| = |Z^y|) = \mathbb{1}(Y_A = \{L(x)\}_{x \in X}).$$

Therefore, by substituting in (5), we obtain

$$\Pr[\mathbf{X}_A = X \mid \mathbf{T}_A(\mathbf{X}_A) = Z, \mathbf{LC}(\mathbf{T}_A) = C] \propto \mathbb{1}(Y_A = \{L(x)\}_{x \in X}) \Pr[\mathbf{X}_A = X].$$

Then, by Theorem 1,

$$\Pr[\mathbf{X}_A = X \mid \mathbf{T}_A(\mathbf{X}_A) = Z, \mathbf{LC}(\mathbf{T}_A) = C] = \Pr[\mathbf{X}_A = X \mid \mathbf{Y}_A = Y_A].$$

In other words, sampling T from \mathcal{F}_0 uniformly at random is perfectly private. The fact that it does not alter the structure of the labels follows directly from $\mathbf{LC}(T) = \mathbf{LC}(\mathcal{X})$ for every $T \in \mathcal{F}_0$. \square

Proposition 2. Let $\mathcal{F}, \mathcal{F}' \subseteq \text{Sym}(\mathcal{X})$ be two families of encoders such that $\mathcal{F} \subseteq \mathcal{F}'$. Then, it is not generally true that \mathcal{F}' is more private than \mathcal{F} .

Proof of Proposition 2. Let $\mathcal{X} = \{1, 2, 3, 4\}$ with $\mathbf{LC}(\mathcal{X}) = (+ + --)$,

$$\mathcal{F} = \begin{cases} T_1 : (1, 2, 3, 4) \\ T_2 : (2, 1, 3, 4) \\ T_3 : (1, 2, 4, 3) \\ T_4 : (2, 1, 4, 3) \end{cases}, \quad \text{and} \quad \mathcal{F}' = \begin{cases} T_1 : (1, 2, 3, 4) \\ T_2 : (2, 1, 3, 4) \\ T_3 : (1, 2, 4, 3) \\ T_4 : (2, 1, 4, 3) \\ T_5 : (3, 4, 1, 2) \end{cases}$$

Then, \mathcal{F} is *optimal*; indeed it is equal to \mathcal{F}_0 as defined in Theorem 2. But \mathcal{F}' is not, as it has an LC-anonymity list with a single member, T_5 . In fact, whenever T_5 is selected from \mathcal{F}' , Eve can perfectly decode X_A . \square

Theorem 3. Let $\mathcal{F}, \mathcal{F}' \subseteq \text{Sym}(\mathcal{X})$ and $\mathcal{F}' \circ \mathcal{F} = \{T' \circ T : T' \in \mathcal{F}', T \in \mathcal{F}\}$. Then, $\mathcal{F}' \circ \mathcal{F}$ is no less private than \mathcal{F} .

Proof of Theorem 3. Let $T'_A \circ T_A \in \mathcal{F}' \circ \mathcal{F}$ be Alice's encoder. We show that if T'_A is given to Eve, then the scheme is as private as if Alice had sampled her encoder from \mathcal{F} . From the definition of the label configuration function, $\mathbf{LC}(T'_A \circ T_A) = C$ if and only if the i -th elements of C is $C_i = L \circ T_A^{-1} \circ (T'_A)^{-1}(x_i)$. We define $\bar{x}_i = (T'_A)^{-1}(x_i)$, for every $x_i \in \mathcal{X}$, which is essentially a new ordering for \mathcal{X} . Under this new ordering, we denote the label configuration function by $\overline{\mathbf{LC}}(T_A)$. We note that $L \circ T_A^{-1}(\bar{x}_i) = L \circ T_A^{-1} \circ (T'_A)^{-1}(x_i) = C_i$, and therefore, $\overline{\mathbf{LC}}(T_A) = C$. We also define $\bar{Z} = (T'_A)^{-1}(Z)$, (Alice's encoded data under the new ordering). Thus,

$$\Pr[\mathbf{X}_A = X_A \mid \mathbf{T}'_A \circ \mathbf{T}_A(\mathbf{X}_A) = Z, \mathbf{LC}(\mathbf{T}'_A \circ \mathbf{T}_A) = C, \mathbf{T}'_A = T'] = \Pr[\mathbf{X}_A = X_A \mid \mathbf{T}_A(\mathbf{X}_A) = \bar{Z}, \overline{\mathbf{LC}}(\mathbf{T}_A) = C],$$

i.e., the same distribution as for \mathcal{F} alone. Thus, $\mathcal{F}' \circ \mathcal{F}$ is at least as private as \mathcal{F} . Analogous arguments show that $\mathcal{F}' \circ \mathcal{F}$ is also at least as private as \mathcal{F}' .

C Additional experiments

Dataset licenses Both the MIMIC-CXR and CheXpert datasets are publicly available under their own licenses. The MIMIC-CXR and CheXpert datasets are available under the PhysioNet Credentialed Health Data License 1.5.0 license and Stanford University School of Medicine CheXpert Dataset Research Use Agreement respectively.

Computational cost All experiments were conducted using Nvidia Tesla V100 or Nvidia RTX A6000 GPUs. All experiments took between 4-6 hours and were primarily bottlenecked by network bandwidth, as our images were hosted on an NFS server. *NeuraCrypt* models had approximately the same runtime as ViT.

C.1 Evaluating modeling utility

For each diagnosis task and training setting, we also report the AUC on MIMIC-CXR and CheXpert test set individually in Table 3 and Table 4 respectively.

Table 3: Impact of *NeuraCrypt* on chest x-ray prediction tasks across different training settings. All metrics are ROC AUCs across the MIMIC-CXR test set. Combined-Clear and Combined-Private refer to using a single *NeuraCrypt* encoder across the combined MIMIC-CXR and CheXpert datasets and two independent *NeuraCrypt* encoders respectively. Guides of abbreviations for medical diagnosis: (E)dema, (P)neumothorax, (Co)nsolidation, (Ca)rdiomegaly and (A)telectasis.

<i>Model</i>	E	P	Co	Ca	A	<i>Average</i>
Train on MIMIC-CXR						
ViT	88 ± 1	78 ± 3	77 ± 2	88 ± 1	85 ± 1	83
<i>NeuraCrypt</i> -ViT	88 ± 2	81 ± 1	73 ± 2	88 ± 1	84 ± 1	83
Train on CheXpert						
ViT	80 ± 1	70 ± 1	69 ± 4	81 ± 1	77 ± 0	75
<i>NeuraCrypt</i> -ViT	82 ± 1	69 ± 2	72 ± 3	79 ± 1	78 ± 0	76
Train on Combined-Clear						
ViT	89 ± 0	83 ± 1	77 ± 2	88 ± 0	86 ± 0	84
<i>NeuraCrypt</i> -ViT	89 ± 0	82 ± 4	79 ± 1	88 ± 0	85 ± 0	85
Train on Combined-Private						
<i>NeuraCrypt</i> -ViT	90 ± 1	82 ± 2	76 ± 3	88 ± 1	85 ± 1	84

Table 4: Impact of *NeuraCrypt* on chest x-ray prediction tasks across different training settings. All metrics are average ROC AUCs on CheXpert test set. Combined-Clear and Combined-Private refer to using a single *NeuraCrypt* encoder across the combined MIMIC-CXR and CheXpert datasets and two independent *NeuraCrypt* encoders respectively. Guides of abbreviations for medical diagnosis: (E)dema, (P)neumothorax, (Co)nsolidation, (Ca)rdiomegaly and (A)telectasis.

<i>Model</i>	E	P	Co	Ca	A	<i>Average</i>
Train on MIMIC-CXR						
ViT	82 ± 1	61 ± 3	72 ± 2	86 ± 0	82 ± 1	77
<i>NeuraCrypt</i> -ViT	83 ± 1	63 ± 2	71 ± 1	86 ± 0	83 ± 0	77
Train on CheXpert						
ViT	83 ± 1	72 ± 1	74 ± 1	85 ± 1	82 ± 0	79
<i>NeuraCrypt</i> -ViT	85 ± 1	74 ± 0	78 ± 1	85 ± 1	83 ± 0	81
Train on Combined-Clear						
ViT	84 ± 1	71 ± 1	75 ± 2	86 ± 1	84 ± 1	79
<i>NeuraCrypt</i> -ViT	85 ± 0	70 ± 2	78 ± 1	87 ± 0	84 ± 1	81
Train on Combined-Private						
<i>NeuraCrypt</i> -ViT	84 ± 2	71 ± 3	77 ± 2	84 ± 2	82 ± 1	80

C.2 Additional attacks

Adversarial attacks. We conducted additional MMD-based adversarial attacks on *NeuraCrypt* while varying the architecture of T^* . We wished to understand if an over-parameterized T^* , e.g with 2x the width or 3x the width, would have better success in attacking T . For these experiments, we used a hidden dimension of 2048 and a depth of 7 for T , and leveraged a T^* with 2x and 3x the hidden dimension of T . We trained T^* for 25 epochs using the Adam optimizer and an initial learning rate of $1e - 04$. As shown in Table 5, attacks leveraging an over-parameterized T^* failed to uncover T , with a $\frac{T^*MSE}{T^{\#}MSE} > 1$.

Plaintext attack. While we do not assume that our adversary has access to either parallel data or the *NeuraCrypt* encoder in our threat model, we also investigated the robustness of *NeuraCrypt* to plaintext attacks. We hypothesized that given a sufficient amount of parallel data, i.e $(x_i, T(x_i))$ pairs and $x_i \in \mathcal{X}$, an attacker could easily learn T . For this experiment, we leveraged the combined MIMIC-CXR and CheXpert dataset with Cardiomegaly labels, used *NeuraCrypt* encoding with a

Table 5: MSE of MMD-based adversarial attacks on *NeuraCrypt* encodings using an over-parametrized T^* .

Encoding	$T^*\text{MSE}/T_\mu\text{MSE}$
<i>NeuraCrypt</i> -width-2x	4.53 ± 0.05
<i>NeuraCrypt</i> -width-3x	4.57 ± 0.08

depth of 7 and a hidden dimension of 2048, as in prior experiments. We trained an estimated T^* for 50 epochs using the Adam optimizer, an initial learning rate of $1e-04$ and a batch size of 64, and report $\frac{T^*\text{MSE}}{T_\mu\text{MSE}}$ on the test set.

We found that *NeuraCrypt* cannot defend against plaintext attacks, illustrating that the security of our encoding scheme relies on the lack of parallel data. We found that the plaintext attack obtains $\frac{T^*\text{MSE}}{T_\mu\text{MSE}}$ of 0.25 ± 0.002 .

C.3 Permutation encodings.

We hypothesized that for any *NeuraCrypt* encoder $T \in \mathcal{F}$ that maps x_i to $T(x_i)$ for every $x_i \in X$ and a random permutation π , there exists a *NeuraCrypt* encoder $T_\pi \in \mathcal{F}$ that maps x_i to $T(x_{\pi(i)})$ for every $x_i \in X$. For this experiment, we used 128 random samples from the combined Mimic-CXR and CheXpert dataset with cardiomegaly labels, and used a *NeuraCrypt* encoding with a depth of 7 and hidden dimension of 2048. We trained T_π for 1000 epochs to minimize $\text{MSE}(T(X), T_\pi(\pi(X)))$ using the Adam optimizer, an initial learning rate of $1e-04$ and a batch size of 64 and report $\frac{T^*\text{MSE}}{T_\mu\text{MSE}}$ on 128 random samples.

We found that T_π could easily learn a mapping from X to a randomly permuted Z . In this experiment, we found T_π obtained an $\frac{T^*\text{MSE}}{T_\mu\text{MSE}}$ of 0.56 ± 0.020 . We note that our permutation encoding experiment only included 128 random samples, and it is unclear at what dataset size a fixed-size T is no longer able to represent arbitrary X to Z bijections.